JOURNAL OF MATERIALS SCIENCE 33 (1998) 3927–3934

Diffusion-based microalloying of aluminium alloys by powder metallurgy and reaction sintering

D.P. BISHOP*, J.R. CAHOON‡, M.C. CHATURVEDI‡, G.J. KIPOUROS*, W.F. CALEY**
* *Department of Mining and Metallurgical Engineering, Technical University of Nova Scotia, Halifax Nova Scotia, Canada B3J 2X4*
** *Department of Mining and Metallurgical Engineering, Dal Tech, Dalhousie University, 1360 Barrington St., Halifax, Nova Scotia, Canada B3J 2X4*
‡ *Department of Mechanical and Industrial Engineering, University of Manitoba, Winnipeg, Manitoba, Canada R3T 5V6*
Email: caleywf@tuns.ca

A diffusion-based technique of microalloying aluminium powder metallurgy products was examined to expand the range of feasible alloying additions. Thermodynamic calculations and diffusion rates for several elements suggested that tin and silver were the most promising; these elements were successfully alloyed into AA 2014 on both a macroscopic and a microscopic scale. The final microstructures were examined using X-ray diffraction, X-ray mapping and energy-dispersive electron probe microanalysis. Silver additions were homogeneous throughout the alloy microstructure, whereas tin was concentrated in intergranular regions only. The results suggested that the technique was viable for a variety of microalloying elements. Also, the extent of alloying was predicted reasonably well using a mathematical mass balance model.

1. Introduction

In light of the many attractive properties offered by aluminium (low density, high strength to-weight ratio and resistance to corrosive environments) the usage and development of alloys based on this element have long been pursued. Although each particular application dictates that certain properties are inevitably of greater concern than others, it is the mechanical properties that are most frequently questioned. As a consequence, a great deal of effort has focused on improving such properties. Whereas property enhancements for a given alloy chemistry can be achieved through appropriate heat treatments, working and thermal mechanical processing, manipulation of bulk alloy chemistry has been the most popular to examine. Commonly, additions of Cu, Si, Mg, Zn, Li and Mn, to an Al base are made of the order of one to several weight per cent in a wide range of combinations [1]. Although these elements dominate in the determination of overall alloy properties, subsequent smaller "trace additions" (i.e., 0.1 at%) of additional elements can also have a pronounced influence. Several main effects of trace element additions have been established [2].

(i) They may induce or remove intercrystalline brittleness by interacting with grain boundaries and reduce or increase interfacial energies in the solid state.

(ii) They may alter the morphology of secondary phases growing from a liquid.

(iii) They may form stable primary phases so as to refine cast grain structure and to control recovery and recrystallization processes.

(iv) They may alter the age-hardening response through a modification of precipitate size and distribution, crystal structure and/or chemistry, often resulting in improved strength.

As a means of achieving the many possible benefits of trace element addition to aluminium, Ti, Zr, Ca, Sr, Na, Ag, Li, Sn, Cd and In are commonly incorporated. Trace additions of Ti and Zr are known to form stable intermetallics of the form MAl_3 (where M = Ti or Zr) which results in possible refinement of the cast grain size and enables recovery and recrystallization behaviour to be controlled [2–4]. The addition of trace amounts of Sr, Na or Ca in levels of the order of 0.01 wt % [5] is known to alter the morphology of secondary phases such as primary silicon, resulting in improved mechanical properties [6] and fatigue resistance [7]. Requiring more attention, however, is the variety of possible manipulations of age-hardening response exerted on certain alloy systems by trace additions of Cd, In, Sn, Ag, Be or V.

In many instances the standard precipitation sequence common to an aluminium alloy may be modified so as to enhance the nucleation frequency of precipitating phases (enhancement of θ' formation in Al–Cu alloys by Cd, In and Sn [2–10], S formation in Al–Li-based alloy 8090 by Be and V [11], and η' formation in Al–Zn–Mg alloys by Ag [2, 10]). As

a consequence, a much finer distribution of the strengthening precipitate results, in some cases significantly narrowing the detrimental precipitate free zones which commonly exist along grain boundaries [10]. In alloy systems such as Al–Cu–Mg and Al–Cu–Li–Mg, the precipitation behaviour can actually be altered to a point where the dominant strengthening precipitate becomes entirely new, differing in crystal structure and frequently, habit plane and chemistry. This dramatic effect has been achieved through trace additions of Ag to Al–Cu–Mg–Li, which promotes the formation of T_1 precipitates, deemed responsible for the high strength levels attained in Weldalite 049™ alloy [12]. In other cases, similar scale Ag additions to Al–Cu–Mg-based alloys of high Cu-to-Mg ratio have resulted in a transformation of θ' to a precipitate referred to as Ω [13–15], of improved hardness and elevated temperature strength [16].

In all cases reviewed to date, trace element additions have been made through standard ingot metallurgy (I/M) practices, whereby a relatively expensive master alloy (binary alloy of Al plus several weight per cent of the trace element) is added to a large melt. In several recent publications, however, the potential of an alternative method of microalloying powder metallurgy (P/M) products has been presented [17–19]. Using this technique, a standard P/M procedure of cold isostatic pressing, sintering and extruding–cold working has been augmented in that a thin outer shell comprised of an alloy–mineral mixture is pressed over a previously pressed alloy substrate, followed by normal sintering and extrusion practices. Using an appropriate mineral, the elevated temperature associated with sintering promotes chemical reaction(s) between the alloy and mineral components of the outer shell, thus reducing the mineral species *in situ* and liberating the required trace element. In response to the activity gradient of this element that exists between the outer shell and central core regions, and the elevated temperature of sintering, a net flux inwards results, principally via intergranular migration. As this microalloying technique is diffusion based, a sintering temperature slightly above the solidus is employed so as to accelerate the microalloying rate. Owing to solid solubility limits [20], some elements modify intergranular (once liquid) regions exclusively (e.g., Ca and Sn), whereas others also interact with the aluminium grains themselves (e.g., Ag).

The aim of this contribution is to expand the domain of potential applications of the process by identifying the most feasible trace element additions to focus on, through consideration of process parameters such as mineralogical sources of the microalloying elements, thermodynamics of alloy–mineral interactions, and diffusion rates of the selected elements in aluminium. For demonstration purposes, Li, Sn, Ca, Ag, Ti and Zr are considered; these elements are all important in microalloying aluminium, their use depending upon the intended structural–mechanical modification desired.

The minerals and compounds chosen as a source for each of the elements of interest are cassiterite (Sn), wollastonite (Ca), spodumene (Li), rutile (Ti), zircon sand (Zr) and silver nitrate (Ag). Of these, cassiterite, wollastonite, spodumene and silver nitrate have been successfully used to date as a source material to microalloy aluminium. Rutile has also been evaluated but found to be too thermodynamically stable at the sintering temperatures used to be successful as a source of Ti.

The following sections outline both the thermodynamic stability of these potential microalloying candidates over the temperature range of interest (773–913 K), and the expected diffusion rates for each in an aluminium matrix. Also, some experimental results for two microalloying elements, namely, Sn from cassiterite and Ag from $AgNO_3$, are presented, together with a mass balance model developed to predict final trace element concentrations from starting mineral–compound composition and concentration.

2. Materials

As a basis for all experiments, a standard commercial aluminium alloy 2014 (AA 2014) (Al–4.4 Cu–0.8 Si–0.8 wt % Mn–0.5 wt % Mg) was utilized. The chemical composition was verified to be within the allowable limits [1]. The alloy powder was supplied by Valimet, located in Stockton, CA produced through inert-gas atomization and had a particle size of -325 mesh. Naturally occurring cassiterite (SnO_2) was selected as a source of Sn. However, the mineral proved difficult to obtain after closure of the only North American operation in Nova Scotia, Canada. Hence, reagent-grade SnO_2 was purchased from Fisher Scientific, having a purity of 99.9% (metals basis) and a particle size restricted to -200 mesh. Silver nitrate ($AgNO_3$) was likewise purchased from Fisher Scientific, it too having a purity of 99.9%.

3. Experimental procedure

In order to produce both unmodified (standard) AA 2014 samples, and samples of AA 2014 microalloyed with additions of Sn and Ag, a previously developed technique [17–19] was employed. In essence, the procedure was based on common P/M practices with an additional ball milling–isostatic pressing sequence. The production of standard unmodified specimens consisted of cold isostatic pressing (190 MPa) alloy powder into cylindrical green bodies (of 20 mm diameter and 150 mm length) followed by liquid-phase sintering at 873 K under flowing high-purity argon, and cold swaging–annealing into a product of nearly theoretical density. In the microalloying technique, the procedure was similar, except that a thin (about 1–2 mm thick) outer shell, consisting of a AA 2014–mineral (or compound) mixture is isostatically pressed over the green body, again at 190 MPa prior to sintering. Microalloying mixtures consisted of 0.05–0.1 mol of the desired mineral or compound per 100 g of AA 2014 powder, dry milled in air for 24 h with several drops of dispersant (50 : 50 acetic acid : methanol mixture [21]) using a ceramic ball mill. These composite green bodies were then liquid phase sintered for various lengths of times, leaving a dense

(96–97% theoretical density) central microalloyed core surrounded by a porous outer shell. After sintering, this shell layer was readily chipped free from the dense microalloyed AA 2014 core. Subsequent cold swaging–annealing operations were thus restricted to the modified AA 2014 core only; final densities approached theoretical values.

Each sample produced using this technique was characterized through scanning electron microscopy (JEOL JSM 840), energy-dispersive electron probe microanalysis (EPMA) using standardless correction (20 kV; 0.3 nA probe current; 120 s scan time; NORVAR™ window), and X-ray diffraction (XRD) (Rigaku™ diffractometer using Cu Kα radiation, and operating parameters of 40 kV, 40 mA and a scan speed of $4^{\circ}/\text{min}^{-1}$). These were used in an effort to assess the extent of mineral–compound dissociation, as well as the location and approximate amount of alloying addition diffused into the central core.

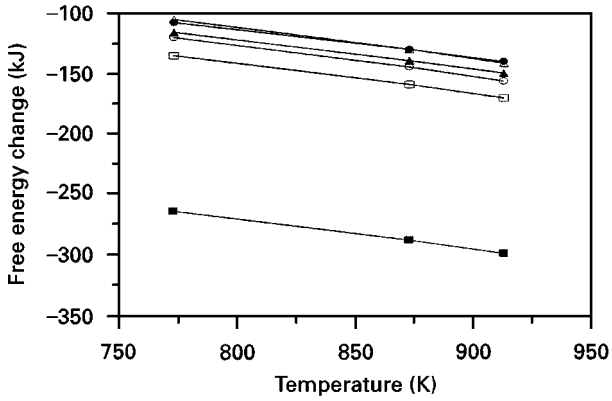

Figure 1 Calculated values of free energy change as a function of temperature. The reactants in each case were 100 g of AA 2014 plus 0.1 mol of the various trace element source compounds. ((□) AA 2014–SnO_2; (△), AA 2014–$CaSiO_3$; (○), AA 2014–(Li–Al–Si 206); (●), AA 2014–TiO_2; (▲), AA 2014–$ZrSiO_4$; (■), AA 2014–$AgNo_3$.

4. Theoretical considerations

In order to introduce the required alloying addition, the technique as developed relies on two stages: firstly the dissociation of the alloying element source mineral or compound and secondly subsequent diffusion of the liberated element into the central alloy core. In an effort to determine which of the selected minerals and compounds were most amenable to processing, the chemical thermodynamic behaviour and diffusion rates of the elements of interest in Al were evaluated. Each of these aspects is discussed in the following two sections.

4.1. Chemical thermodynamics

Prior to diffusing into the alloy, the trace element of interest must first be dissociated from its source compound. Thus, any insight into the tendency for this reduction is invaluable and, as a means of assessment, one must consider the governing thermodynamic principles.

A thermodynamic software package , F* A* C* T*™ (Facility for the Analysis of Chemical Thermodynamics) [22] was employed to provide the thermodynamic calculations. Using this package, the user is prompted to input the appropriate reactants in their respective amounts together with temperature and pressure. As output, a list of the most plausible reaction products, together with a variety of thermodynamic data (including a calculation for the overall free energy change) is given. On the basis of these data, one could readily identify which of the candidates were most likely to be reduced into a form suitable for subsequent diffusion.

Using F* A* C* T*™, the dissociation of each compound in the presence of AA 2014 was studied. In all calculations, the reactants input included 100 g of AA 2014 together with 0.1 mol of the mineralogical, oxide or nitrate compounds outlined in the previous section. The results are shown in Fig. 1 and Table I. As shown in Fig. 1, thermodynamic predictions indicated that all the chosen minerals and compounds had a reasonable tendency for dissociation; relatively speaking, $AgNO_3$ possessed the largest, cassiterite was intermediate, whereas wollastonite and rutile displayed the weakest.

Aside from predictions into the tendency to react, those pertaining to the anticipated reaction products (Table I) are also of use. Intuitively, one may expect that, should the liberated alloying element react to form a stable solid compound(s), its ability to diffuse into the central alloy core would be lessened. Conversely, if this element tends to concentrate within the liquid phase in a soluble manner, the formation of stable solid compounds is avoided, and an increased amount is available for diffusion. Using this information, it appears that, once liberated, Ca, Sn, Li and Ag should be readily available for diffusion into the central core.

4.2. Diffusion

Once the element of interest has been liberated from its starting compound, the existence of a chemical potential gradient coupled with an elevated temperature promotes diffusion-based alloying of the central AA 2014 core. Since alloying predominantly occurs during liquid-phase sintering, one must consider diffusion rates not only in the solid phase but also those in liquid metal. Values for diffusion rates in solid aluminium were compiled from the literature and are given in Table II. Although a variety of rates have been measured for most of the binary systems considered, the values cited in the table are deemed representative. No experimental data were found for the diffusion of Ca and Ti in Al; hence, the calculated values from the model developed by Burachynsky and Cahoon [23] are included. As shown in the table, Ca appeared to possess the fastest rate whereas that of Sn was second, Ag, Ti and Li are all about six times slower than Sn, and that of Zr was about five orders of magnitude slower again. As the anticipated diffusion rates differed by some six orders of magnitude, introduction of the required element into the solid constituent during sintering should vary considerably. However, diffusion into the liquid phase is expected to be

TABLE I
Summary of the main reaction products predicted by F * A * C * T™, where the reactants in each case were 100 g of AA 2014 plus 0.1 mol of the respective trace element source compound

Trace element source compound	Predicted reaction products		
	Gaseous	Liquid	Solid
Rutile (TiO_2)	None	Al–Cu–Mn–Si	Al, $TiAl_3$, Al_2O_3, $MgAl_2O_4$, TiSi
Zircon sand ($ZrSiO_4$)	None	Al–Cu–Mn–Si	Al, ZrSi, Al_2O_3, $MgAl_2O_4$
Spodumene ($LiAlSi_2O_6$)	None	Al–Cu–Si–Mn–Li	Al, Al_2O_3, $LiAlO_2$, Si, $MgAl_2O_4$, $Mn_{10}Si_{17}$
Wollastonite ($CaSiO_3$)	None	Al–Ca–Cu–Si–Mn	Al_2O_3, $MgAl_2O_4$, Si
Cassiterite (SnO_2)	None	Al–Sn–Cu–Mn–Si	Al, Al_2O_3, $MgAl_2O_4$
$AgNO_3$)	None	Al–Ag–Cu–Mn–Si	Al, Al_2O_3, AlN, $MgAl_2O_4$

TABLE II
Summary of diffusion rates in solid aluminium at temperatures of interest [22]

Element	$D_{773\,K}$ ($m^2\,s^{-1}$)	$D_{873\,K}$ ($m^2\,s^{-1}$)	$D_{913\,K}$ ($m^2\,s^{-1}$)
Al (experimental)	4.06×10^{-14}	5.10×10^{-13}	1.20×10^{-12}
Ca (calculated)	2.63×10^{-11}	1.68×10^{-10}	3.14×10^{-10}
Sn (experimental)	8.13×10^{-13}	6.73×10^{-12}	1.38×10^{-11}
Ag (experimental)	1.56×10^{-13}	1.26×10^{-12}	2.56×10^{-12}
Li (experimental)	1.07×10^{-13}	1.01×10^{-12}	2.16×10^{-12}
Ti (calculated)	1.13×10^{-13}	1.35×10^{-12}	3.12×10^{-12}
Zr (experimental)	3.23×10^{-18}	2.41×10^{-16}	1.04×10^{-15}

significantly different. It is well known that diffusion rates in molten metals are much higher than those in solids and typically range between 10^{-9} and 10^{-8} $m^2\,s^{-1}$, regardless of the element under consideration [24]. In this light, it is expected that the preferential diffusion path would be through the liquid component, with all elements having a similar likelihood of being alloyed into the central alloy core.

5. Experimental results

On examination of the theoretical considerations for the candidates selected (Tables I and II and Fig. 1), the two compounds believed to be the most amenable for microalloying by this technique are cassiterite (SnO_2) and ($AgNO_3$). Hence, the majority of experimental results detailed pertain to these.

As described, mixtures of AA 2014 powder and the two compounds were mixed and sintered for various lengths of time ranging from 0.5 to 16 h. Resulting compacts were examined using optical metallography, EPMA and XRD.

XRD results for AA 2014–$AgNO_3$ and AA 2014–SnO_2 sintered for various lengths of time are presented in Fig. 2. Regarding the AA 2014–$AgNO_3$ system (Fig. 2a), diffraction peaks associated with the nitrate appeared strong in the unsintered mixture; yet these peaks were absent in scans conducted after sintering, indicating complete dissociation. As shown in Fig. 2b, SnO_2 had also dissociated during sintering, as is evident from a substantial reduction in the amplitude of its characteristic peaks, and the subsequent emergence of peaks characteristic of metallic Sn. However, it appears that the extent of dissociation was not as complete as that with $AgNO_3$ owing to the retention of small SnO_2 diffraction peaks through all sintering times considered. The trend of decreasing extent of dissociation was consistent with their respective tendencies to dissociate as thermodynamically predicted. The tendency for dissociation was also assessed in previous experiments using wollastonite [17–19] and, recently, rutile. Experiments on AA 2014–wollastonite mixtures verified that this mineral dissociated after sintering, consistent with the thermodynamic predictions. Somewhat in contrast with this trend, however, were recent results for mixtures of AA 2014 and rutile. Whereas it was thermodynamically predicted that this mineral should behave in a manner similar to that of wollastonite, results indicated that this compound had in fact undergone no dissociation after sintering.

As both $AgNO_3$ and SnO_2 dissociated during sintering, the sintered core products were examined using EPMA in an attempt to verify the extent and location of diffusion of microalloying elements. X-ray maps generated for AA 2014 microalloyed with Sn and Ag using a sintering time of 16 h are shown in Figs 3 and 4. In general, the microstructure of standard AA 2014 was comprised of alloy grains and intergranular regions, a detailed chemical analysis of which has been given elsewhere [18]. Briefly, alloy grains had a composition similar to that of the bulk alloy, whereas the intergranular regions were enriched in alloying elements, the principal of which was Cu. Regarding the Ag-modified sample, results indicated a homogeneous distribution of Ag between alloy grains and intergranular regions. Cu, however, was also found throughout the sample and yet was more concentrated in intergranular regions. For the Sn-modified sample, results showed that Sn was concentrated in the intergranular regions only, whereas Cu exhibited a similar type of distribution to that found in Ag-modified samples. Studies at higher magnifications revealed that Sn had behaved in an inert manner with respect to other elements concentrated in these regions, failing to form intermetallics, and remained as

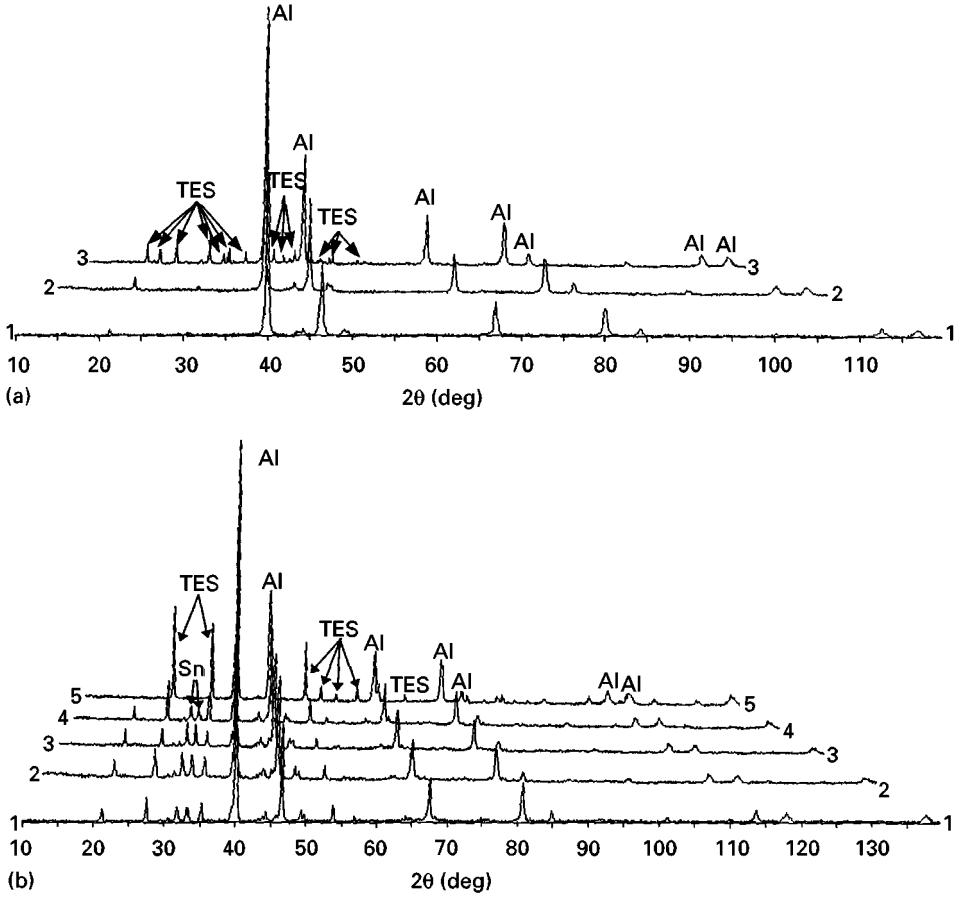

Figure 2 XRD scans conducted on sintered mixtures of (a) AA 2014–$AgNo_3$ (scans 1,2 and 3 denote sintering times of 16 h, 4 h and 0 h, respectively) and (b) AA 2014–SnO_2 (scans 1, 2, 3, 4 and 5 denote sintering times of 4, 2, 1, 0.5 h and 0 h, respectively). Al, Sn and TES indicate peaks for aluminium, tin and trace element source ($AgNO_3$ in (a) and SnO_2 in (b)).

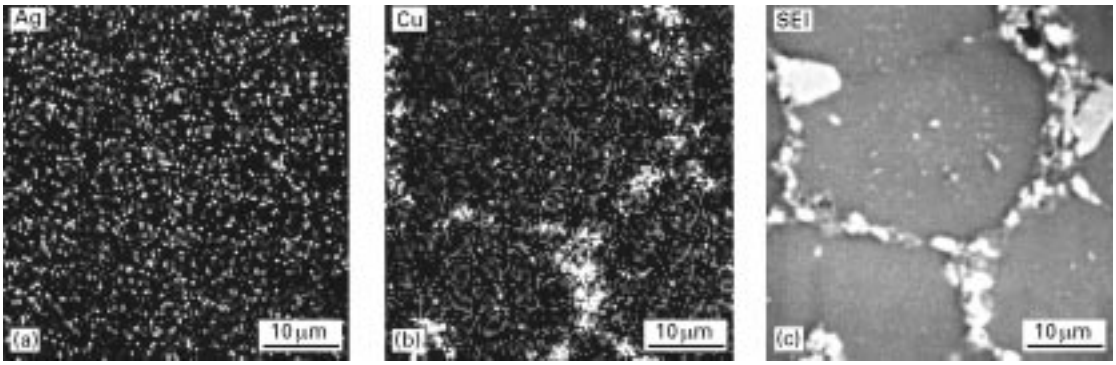

Figure 3 X-ray maps compiled for Ag-modified AA 2014: (a) Ag scan; (b) Cu scan; (c) corresponding secondary-electron image (SEI).

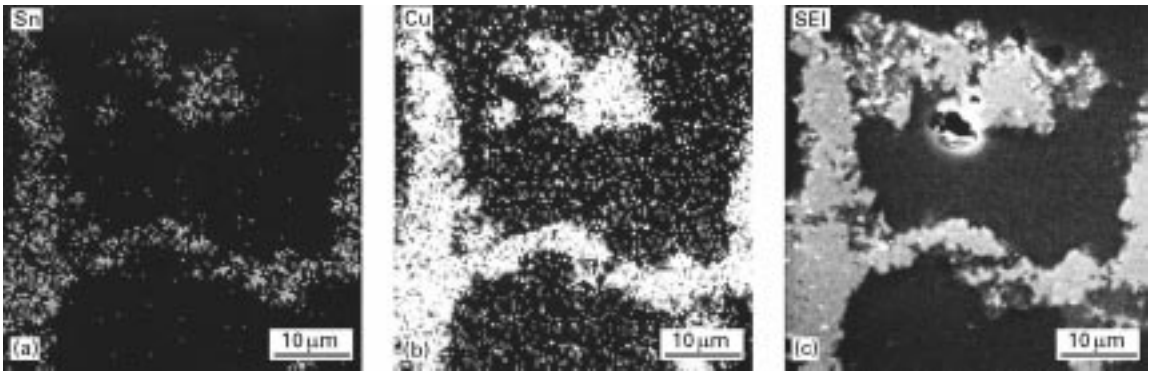

Figure 4 X-ray maps compiled for Sn-modified AA 2014; (a) Sn scan; (b) Cu scan; (c) corresponding secondary-electron image (SEI).

pure Sn. In previous work [17–19], Ca was found to have a distribution within the microstructure similar to that of Sn. However, owing to the very small size of Ca-based particles, it was not possible to determine whether Ca was present as a pure metal, intermetallic or oxide using EPMA. Despite additional efforts using transmission electron microscopy, identification of the Ca-based particles remained inconclusive owing to the preferential attack and fall out of intergranular regions during sample preparation.

Quantitative results for Sn and Ag contents of samples sintered for various lengths of time are presented in Fig. 5. All values reported in the figure were determined using large-scale energy-dispersive EPMA scans and standardless correction. Although some measurements approached the lower limit of detection for the instrument, the results were reproducible and deemed reasonable since, more accurate, wet chemical analyses of several of the same samples indicated similar concentrations. To confirm these results, tests conducted on AA 2014 standard unmodified samples, showed Ag and Sn concentrations to be less than 0.05 wt%. Although not shown in the figure, Ca concentrations (from dissociation of wollastonite) were measured to be approximately 0.02 at% after sintering for 16 h.

To model the extent of alloying in a quantitative manner, a computer program was developed that allowed input of process variables such as core size, shell thickness, aluminium alloy and alloying element (together with its respective source compound and starting concentration in the blended shell powder). From a thermodynamic perspective, the inward diffusion of an alloying element should continue until an equal chemical potential for the species exists in both the shell and the core components. To model this situation accurately, data on the activity and activity coefficients of the element in AA 2014 are thus required. However, owing to the limited availability of such data, the program was written assuming ideal behaviour. Consequently, the activity of any given element is assumed to be equal to its respective mole fraction, thus defining equilibrium as the point of equal concentrations rather than chemical potentials.

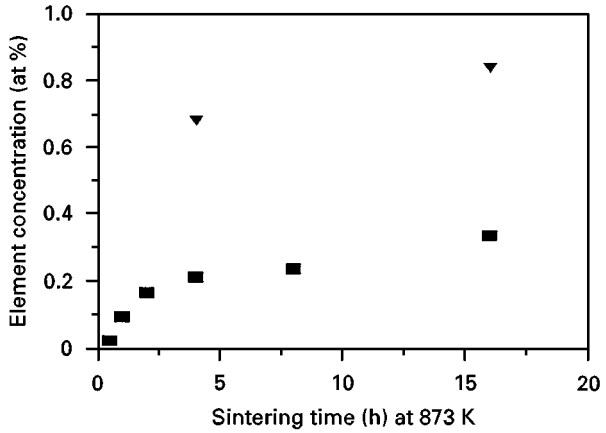

Figure 5 Approximate concentrations of Sn (■) and Ag (▲) in modified and unmodified alloy AA 2014 samples determined by wet chemical analyses and large-scale energy-dispersive EPMA scans.

Although the greatest portion of the alloying addition should diffuse into the core, some must remain in the shell to satisfy equilibrium conditions. To model this situation, plots of core and shell concentration versus the fraction of alloying addition diffused into the core were produced for Ca, Ag and Sn (Fig. 6) using measured dimensions and starting concentrations corresponding to actual samples. The intersection point of the two lines represented the equilibrium concentration expected together with the efficiency of alloying

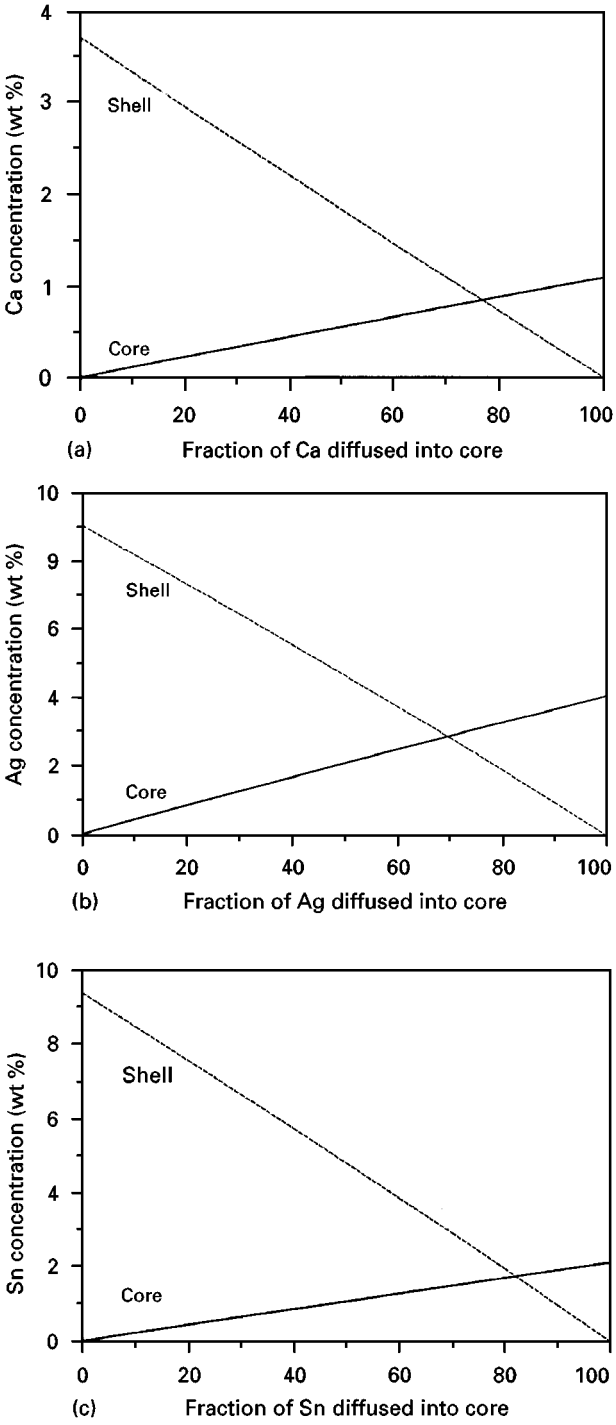

Figure 6 Calculated concentrations of microalloying addition in core and shell components as a function of the fraction of element diffused: (a) Ca (AA 2014 core; AA 2014 + 0.1 mol of $CaSiO_3$ shell; shell thickness of 1.8 mm, core diameter of 2.5 cm); (b) Ag (AA 2014 core; AA 2014 + 0.1 mol of $AgNO_3$ shell; shell thickness of 1.8 mm, core diameter of 1.8 cm); (c) Sn (AA 2014 core; AA 2014 + 0.1 mol of SnO_2 shell; shell thickness of 1.1 mm, core diameter of 2.1 cm);

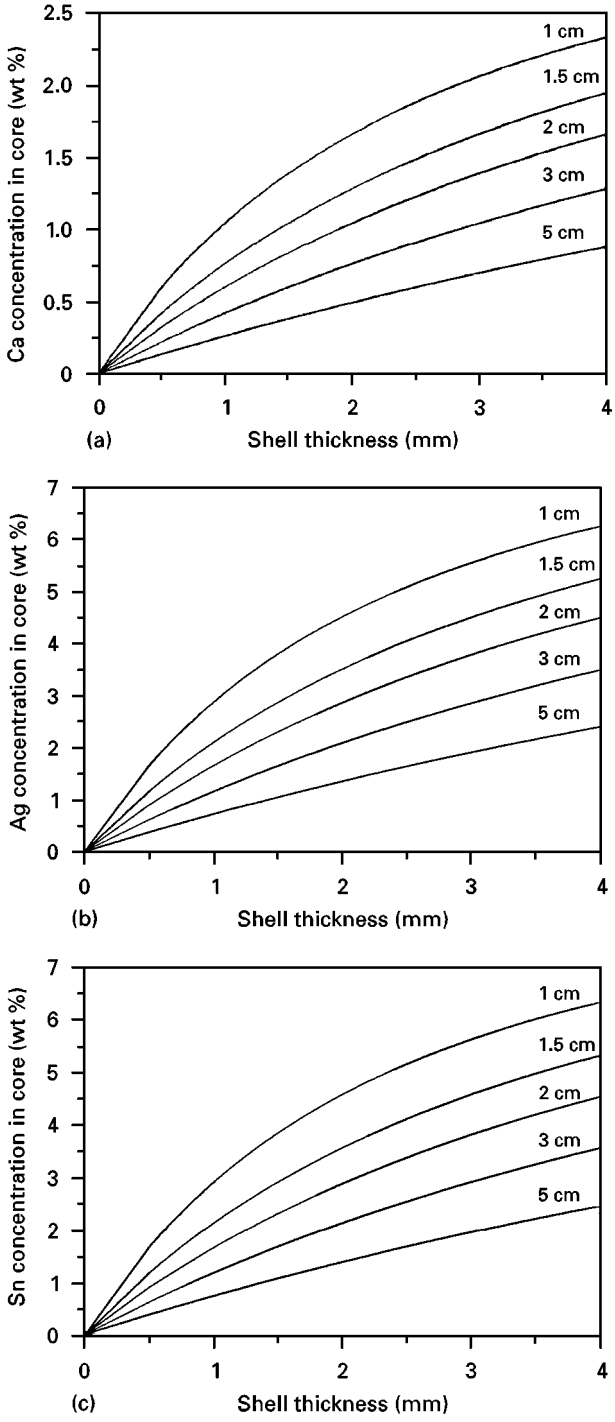

Figure 7 Calculated equilibrium concentrations of various microalloying elements as a function of shell thickness for different sized cores (sintered diameters are shown on the right-hand side of each plot) : (a) Ca; (b) Ag; (c) Sn.

element usage. Further extension of the model to account for varying shell thickness and core diameters (Fig. 7) revealed that a significant range of microalloying is attainable with minimal variation in shell thickness.

6. Discussion

Several possible microalloying additions were initially evaluated on the basis of chemical thermodynamics and diffusivity considerations. In the case of thermodynamics, it was found that all candidates have a tendency to dissociate during sintering, some more so than others. In an effort to assess the validity of these predictions, actual alloy–mineral (compound) mixtures were sintered and examined. With respect to the extent of dissociation, results showed $AgNO_3$ to be complete, SnO_2 and wollastonite close to completion, and yet rutile was completely unaffected. Whereas the trend of increasing dissociation tendency from wollastonite to SnO_2 to $AgNO_3$ was thermodynamically predicted, the inert nature of rutile was not. This illustrates that, in order to predict correctly the reactions which may occur in any system, one must address both thermodynamics and kinetics. Thus, the discrepancy mentioned was probably a result of relatively sluggish reaction kinetics for rutile.

As the desired alloying addition was made via diffusion, the diffusion rates of candidate elements in Al were considered. For the three elements of principal interest, decreasing diffusivities in solid Al from Ca to Sn to Ag were anticipated. Intuitively one might expect the same order of decreasing alloying element concentrations in central alloy cores for any given sintering time. However, the opposite was discovered, probably the result of several contributing factors. First, since liquid-phase sintering was utilized, the liquid component offered a preferential path of high diffusivity for any element introduced into the core. During sintering at 873 K, an Al-trace element liquid phase will form with Ag, Sn and Ca; this facilitates permeation (alloying) into the mushy alloy core. On this basis, it is postulated that trace elements which do not form a liquid region when alloying with Al (i.e., Ti and Zr) at 873 K may not permeate the alloy core as readily. Thus, as Ag Sn, and Ca were expected to have similar diffusion rates through the liquid phase, the larger differences between solid diffusivities may not have been fully reflected in the final concentration of the element reached.

Another contributing factor is the concentration of the trace element in the phase contacting the alloy particles since a higher concentration would tend to result in a more rapid distribution of the trace element throughout the alloy core. At the sintering temperature of 873 K, and considering binary [20] systems only, the contacting phase for Ag and Sn would be a liquid containing about 50 wt% Ag or 50 wt% Sn, respectively. For the trace element Ca, the phase contacting the alloy particles would be solid Al_4Ca, containing about 28 wt% Ca. After sintering for 16 h, both Sn and Ca are concentrated in the intergranular regions, which for AA 2014 were once liquid, whereas Ag is homogeneously distributed throughout the core microstructure. Since both Sn and Ca diffuse faster than Ag in Al (Table II), it is reasonable to assume that these two trace elements would also be distributed throughout the entire core microstructure. However, since their solid solubility limits in Al (less than 0.01 wt% and 0.1 wt% for Ca and Sn, respectively) are below the resolvable limits of EPMA, this assumption could not be verified.

As revealed in XRD scans of the shell component, the reduction of $AgNO_3$ was complete, whereas that of SnO_2 was not. Consequently, the concentration of

atoms available for inward diffusion is substantially greater for Ag than for Sn, leading to a correspondingly higher concentration gradient, and in turn driving force, for diffusion. In response, the inward flux of Ag should be greater than Sn, as shown by the higher concentrations achieved.

Assays of core alloy chemistry indicated that the amount of diffusing species introduced varied with sintering time. Evidently, both microscopic and macroscopic scale alloying could be achieved, provided that an appropriate sintering time was selected. Although the change in concentration was found to be relatively steep for short sintering times, a trend to a plateau developed as sintering continued, suggesting an approach towards equilibrium. Comparing calculated results with the concentrations measured in samples sintered for 16 h indicated a reasonable correlation. For example, calculated concentrations of Ag and Sn were 2.9 wt% and 1.8 wt% respectively, whereas measurements indicated 2.8 wt% and 1.4 wt% respectively. Thus, despite the simplicity of this approach, a reasonable estimation of the final concentration was possible.

Although AA 2014 was the sole alloy of interest in this report, it is believed that the process may be applied to many additional aluminium-based alloys. In principle, any aluminium alloy that exhibits a substantial mushy zone (solid plus liquid regime) should be amenable to liquid-phase sintering. The network of liquid that is formed then provides a path for rapid diffusion and thus allows (micro)alloying addition(s) to be introduced in a reasonable period of time.

7. Conclusions

1. Owing to similar diffusions rates in liquid Al, virtually any trace element may be microalloyed into an appropriate aluminium alloy using this technique. However, the formation of an Al-trace element liquid phase at the sintering temperature may be a requirement.

2. Using the technique, macroscopic and microscopic scale alloying additions of Sn and Ag to AA 2014 were possible.

3. The extent of alloying principally depended on the reducibility of the starting compound, the tendency of the addition to form intermetallics, and solid solubility in aluminium.

4. Of the elements considered, Ag was most readily microalloyed.

5. Mass balance calculations can be used to provide reasonable estimates of the trace element concentrations achieved.

Acknowledgements

The authors acknowledge financial assistance from the Natural Sciences and Engineering Research Council of Canada. In addition, the technical assistance of Don Mardis and John Van Dorp at the University of Manitoba is gratefully acknowledged.

References

1. ASM Committee on Aluminium and Aluminium Alloys, in "Metals handbook", Vol. 2 (American Society for Metals, Metals Park, OH, 9th Edn, 1979) pp. 17–21.
2. E. HORNBOGEN and E. A. STARKE, *Acta. Metall. Mater*., **41** (1993) 1.
3. A. R. HARDING, in "Aluminium transformation and technology" (American Society for Metals, Metals Park, OH, 1978) pp. 211–240.
4. A. K. MUKHOPADHYAY, G. J. SHIFLET and E. A. STARKE, *Scripta Metall. Mater*. **24** (1990) 307.
5. R. E. NAPOLITANO, in Proceedings of the Fourth International Conference on Aluminium Alloys, Vol. 1 Atlanta, GA, 1994, Editor: T. H. Sandes, Jr., Georgia Institute of Technology, publ. (1994) p. 99.
6. W. F. SMITH, in "Structure and properties of engineering alloys" (McGraw-Hill, New York, 1981) pp. 206–209.
7. M. SCHAEFER and R. A. FOURNELLE, *Metall. Mater. Trans. A* **27** (1996) 1293.
8. R. SANKARAN and C. LAIRD, *Mater. Sci. Engng*. **14** (1974) 271.
9. S. P. RINGER, K. HONO and T. SAKURAI, *Metall. Mater. Trans. A* **26** (1995) 2207.
10. A. K. MUKHOPADHYAY, G. J. SHIFLET and E. A. STARKE, in Morris E. Fine Symposium, edited by P. K. Liaw, J. R. Weertman and J. S. Satner, (Metallurgical Society of AIME, Warrendale, PA, 1990) pp. 283–291.
11. A. LUO and W. V. YOUDELIS, *Can. Metall. Quart*. **31** (1992) 238.
12. A. R. C. WESTWOOD, *Mater. Sci. Technol*. **6** (1990) 958.
13. I. J. POLMEAR, *Trans. Metall. Soc. AMIE* **230** (1964) 1331.
14. V. D. SCOTT, S. KERRY and R. L. TRUMPER, *Mater. Sci. Technol*. **3** (1987) 827.
15. B. C. MUDDLE and I. J. POLMEAR, *Acta Metall*. **37** 3 (1989) 777.
16. S. P. RINGER, W. YEUNG, B. C. MUDDLE and I. J. POLMEAR, *Acta Metall. Mater*. **42** (1994) 1715.
17. D. P. BISHOP, MASc thesis, Technical University of Nova Scotia, Halifax (1995).
18. D. P. BISHOP, G. J. KIPOUROS and W. F. CALEY, *J. Mater. Sci*. **32** (1997) 2353.
19. D. P. BISHOP, G. J. KIPOUROS and W. F. CALEY, in Proceedings of the International Symposium on Light Metals, Montreal, Quebec, August 1996, edited by M. Avedesian, R. Guilbault, and D. Ksinsik (Canadian Institute of Mining, Metallurgy and Petroleum Montreal PQ Canada, 1996), pp. 525–538.
20. L. F. MONDOLFO, "Aluminium alloys: structure and properties" (Butterworth, London, 1979) pp. 213–380.
21. Personal Communication, Minerals Engineering Centre, Technical University of Nova Scotia, C. Cole, author (1997).
22. W. T. THOMPSON, A. D. PELTON and C. W. BALE, "F*A*C*T* guide to operations," McGill University Press Montreal, PQ Canada (1985) pp. 1–43.
23. V. BURACHYNSKY and J. R. CAHOON, *Metall. Mater. Trans. A* **28** (1997) 563.
24. G. H. GEIGER and D. R. POIRIER, in "Transport phenomena in metallurgy" (Addison-Welsey, Reading, MA, 1973) pp. 458–460.

Received 19 May 1997 and accepted 11 May 1998